Single Molecule Nanometronome

ARTICLE *in* NANO LETTERS · APRIL 2006

Impact Factor: 13.59 · DOI: 10.1021/nl052492p · Source: PubMed

3 AUTHORS, INCLUDING:

Chittanon Buranachai
Prince of Songkla University
11 PUBLICATIONS **573** CITATIONS
SEE PROFILE

Sean A Mckinney
Stowers Institute for Medical Research
21 PUBLICATIONS **3,709** CITATIONS
SEE PROFILE

Published in final edited form as:
Nano Lett. 2006 March ; 6(3): 496–500. doi:10.1021/nl052492p.

Single Molecule Nano-Metronome

Chittanon Buranachai, **Sean A. McKinney**, and **Taekjip Ha**
Center for Biophysics and Computational Biology, Department of Physics, University of Illinois, Urbana-Champaign, and Howard Hughes Medical Institute, Urbana, Illinois, USA

Abstract

We constructed a DNA-based nano-mechanical device called the nano-metronome. Our device is made by introducing complementary single stranded overhangs at the two arms of the DNA four-way junction. The ticking rates of this stochastic metronome depend on ion concentrations and can be changed by a set of DNA-based switches to deactivate/reactivate the sticky end. Since the device displays clearly distinguishable responses even with a single basepair difference, it may lead to a single molecule sensor of minute sequence differences of a target DNA.

DNA-based nano-machines and nano-devices have increased rapidly in popularity in recent years[1–4]. The variety of their forms originates from careful control of molecular recognition between nucleotides, and their functions are based on changes between possible conformations. These conformational changes are in general effected by changes in solution conditions such as ionic strength[5, 6], pH[7, 8] or temperature[9], or by applying short "fuel" oligonucleotides that selectively interact with a specific part of the device[10, 11]. Here we introduce a DNA-based nano-device that undergoes thermally driven structural changes whose switching rate is user controllable. We call our device the "single molecule nano-metronome" because the 'ticking' rates measured from individual nano-devices can be manipulated by magnesium ion concentration and by addition of partially complementary DNA strands.

The nano-metronome can be viewed as the marriage between a "molecular beacon"[12, 13] and the four-way DNA Holliday junction[14]. It is composed of four single-stranded DNA forming a four-way junction with two extra single-stranded overhangs capable of forming basepairs with each other (Figure 1A). In the presence of divalent metal ions such as Mg^{2+} ($\geq$ 100 μM) [15], the Holliday junction folds into compact conformations called stacked-X structures[16]. There are two stacked-X conformers (Figure 1A, *IsoI* : helix H stacks on helix B/helix R stacks on helix X, and *IsoII* : helix B stacks on helix X/helix H stacks on helix R) and single molecule measurements have shown that the two conformers are in continual exchange on the millisecond time scale[17, 18]. The DNA sequence at the strand exchange point dictates how one conformer is preferred over the other[15] and the rates of transition between them strongly depend on the type and concentration of metal ions in solution[17, 18]. In order for the conformational transitions to occur between the two compact conformers, it is thought that the molecule must go through an intermediate open structure (*structure 2* in Figure 1A), which becomes highly populated in the absence of metal ions. However, the open structure can not be directly resolved in magnesium solution even in single molecule measurements, possibly as a result of limited time resolution[17, 18].

Here, we chose a junction sequence (called Junction 7) without any significant conformational bias[17, 19], that is, the lifetimes of the two conformers are similar before imposing external conformational constraints. The addition of two single-stranded overhangs at the end of two

Correspondence should be addressed to T.H. (tjha@uiuc.edu).

helical arms (helix B and H, Figure 1) introduces an extra conformer (*structure 4*), which is similar to *structure 3* but stabilized due to the base pairing of the sticky ends. This extra conformer, likely to have the same global junction conformation (*IsoII*), would force the nano-metronome to preferentially stay in one conformation (*IsoII*) over the other (*IsoI*), hence altering the ticking rates of the nano-metronome. The sequence information of the junction and the overhangs can be found in Supplementary Figure S1.

Real time structural changes of the nano-metronome are monitored at the single molecule level via Förster Resonance Energy Transfer (FRET) using a total internal reflection fluorescence microscope. The donor (Cy3) and acceptor (Cy5) are attached to the ends of helix H and helix B, respectively (Figure 1). As the efficiency of FRET, *E*, scales as a reciprocal of the sixth power of donor-acceptor intermolecular distance R, $E=\frac{1}{1+(\mathbf{R}/\mathbf{R}_0)^6}$[20], upon exciting the donor with a 532 nm laser, the low FRET state (stronger donor emission) corresponds to the junction in *IsoI* (*structure 1*) in which two fluorophores are substantially separated whereas the high FRET states (stronger acceptor emission) represent the junction in *IsoII* (and nano-metronome in either *structure 3* or *structure 4*). The single molecule FRET efficiency, *E*, is approximated by the acceptor intensity divided by the sum of the donor and acceptor intensities.

The presence of the partially complementary overhangs clearly biases the nano-metronomes toward *IsoII* conformer (high FRET), as can be seen from the single molecule FRET time traces of the constructs with 4 bp and 5 bp sticky ends (Figure 2A, top two traces). Even with just a single additional A-T basepair, the bias is significantly enhanced with the 5 bp sticky end compared to the 4 bp. Constructs with 6 bp and 7 bp sticky ends increased the dwell times in the high FRET state even more so that most molecules stayed only in the high FRET state before undergoing photobleaching, precluding detailed analysis (data not shown).

To evaluate the homogeneity of many single molecules of nominally identical metronomes, we made a scatter plot of the average dwell times of the high FRET state vs. the low FRET state in the logarithmic scale (Figure 2B). Each data point in the scatter plot represents a single nano-metronome. The data from nano-metronomes with 4 bp sticky end (red dots, 234 molecules) and with 5 bp sticky end (blue dots, 241 molecules) form distinct clusters, showing that heterogeneity between molecules, either statistical or intrinsic, is small enough to reveal reliably even one base pair difference in the single stranded overhang. The clusters are much more clearly separated along the high FRET state axis than in the low FRET state axis, suggesting that the sticky end plays a much more significant role for *IsoII* as predicted. The low FRET state's average dwell times fall into the same range of that of unconstrained Junction 7[17, 18] indicating that the presence of sticky ends does not drastically affect the dwell time of the *IsoI*.

Figure 2C (top and middle panels) shows that the FRET efficiency of the high and low FRET states is essentially identical for 4 bp and 5 bp sticky ends, $E\sim0.85$. Whether this is because there is no distance difference or because FRET is not very sensitive to small distance differences in this range is not clear.

Next, we studied the effect of Mg^{2+} concentration on the nano-metronome dynamics. Transition rates between two conformers of the Holliday junction depend strongly on the ionic strength. It has been shown[17] that, over a range of sub-millimolar to several hundred millimolar in concentration[17], Mg^{2+} increases the dwell times of both conformers by screening the electrostatic repulsion between the phosphate backbones at the strand exchange point, thereby stabilizing the stacked conformations. Figure 3A and 3B show that, for the nano-metronomes too, the dwell times of both the high FRET state and the low FRET state increase as the concentration of Mg^{2+} is raised (Mg^{2+} concentration = 5, 10, 30, and 50 mM). The deviation

from the solid reference line, which represents where the data from normal Junction 7 is located (a 1:1 ratio of high FRET and low FRET dwell time), is due to the selective stabilization of the high FRET state by the sticky end. Not surprisingly, at the same salt concentration, the 5 bp sticky end (Figure 3B) yields a larger deviation from the reference line than the 4 bp sticky end (Figure 3A).

The increase in Mg^{2+} concentration also slightly raises the FRET efficiency of the high FRET state in both cases (Figure 3C and 3D). We discovered that in the case of junction 7, the high FRET peak values were also raised by the increasing Mg^{2+} concentration (data not shown) possibly due to a stronger screening of the high salt concentration at the strand exchange point resulting in the closer distance between the FRET pairs. This may be what is happening in the case of the nano-metronome as well. Another possible reason here is that Mg^{2+} also enhances the stability of the basepairing at the sticky end, making *structure 4* relatively more populated than *structure 3*. It has been shown that a 5 bp sticky end (5′ CCCAA---TTGGG 3′) within a molecular beacon undergoes sub-millisecond zipping-unzipping transitions and the equilibrium shifts to the zipped state with increasing salt concentration[13]. If this is applicable to our case, the apparent FRET efficiencies we obtain may be a result of time-averaging over multiple transitions between *structure 3* and *structure 4* within our time resolution (30 ms); the longer the nano-metronome stays in *structure 4* at higher Mg^{2+} concentrations, the higher the measured apparent FRET efficiencies. Another interesting observation is that Mg^{2+} stabilized the 5 bp sticky end more strongly than it did for the 4 bp sticky end, as can be seen from the higher slope in the scatter plot (Figure 3A and 3B).

Next, we introduce a mechanism to change the ticking rates of our nano-metronome. The idea, as applied to various types of DNA-based nano-scaffolds[10, 11] and nano-machines[1, 2, 21], is based on two different, but fully complementary, short single stranded DNA we call the deactivator and activator. The deactivator is capable of forming stable basepairing with the single-stranded overhang at the end of helix H. This deactivator binding silences the sticky end, turning the nano-metronome into a normal Junction 7 (Figure 1B). The reaction can be reversed by applying the activator. After the binding of the activator to the exposed region of the deactivator, a triple-stranded branch migration occurs, and eventually the deactivator leaves the sticky end because of the formation of full duplex DNA between the activator and the deactivator which is energetically more stable. Afterward, the nano-metronome returns to the original state (Figure 1A).

A sample trace from a silenced nano-metronome (Figure 2A, bottom trace) clearly exhibits the much higher transition rates between the high FRET and low FRET states compared with those from nano-metronomes with 5 bp and 4 bp sticky ends. Figure 2B compares the high FRET and low FRET dwell times of the nano-metronomes (4 bp version) with deactivated sticky ends (green dots, 85 molecules) to the nano-metronomes having active 4 bp (red dots) and 5 bp (blue dots) sticky ends. The silenced sticky end yields an approximate 1:1 high FRET and low FRET dwell time as expected from a normal Junction 7. The single molecule FRET histogram for the deactivated nano-metronome (4 bp version) (Figure 2C, the bottom plot) shows two peaks with comparable populations. The FRET value of the high FRET state (E~0.65) is lower than that of 4 bp and 5 bp sticky ends and is similar to what was reported from Junction 7 previously[17]. Thus, not only do the sticky ends bias the nano-metronome toward *IsoII*, they also raise the apparent FRET efficiency of the high FRET state from 0.65 to 0.85 (Figure 2C). If the FRET increase is due to distance decrease, this would indicate that the Holliday junction is relatively flexible and a range of inter-helical angles may be allowed within each stacked conformation. It is likely that the length of the overhangs will influence the FRET values of the nano-metronome when the stick end has been basepaired.

Figure 4 shows that we can observe the sudden change in the ticking rate of a single nano-metronome when the deactivator or the activator strands are added. Here the deactivation/re-activation of the sticky end is monitored in real time using a flow delivery system. In Figure 4A, the time trace starts with a nano-metronome having an active 5 bp sticky end. At approximately t = 30 sec, a high concentration (~ 1 μM) of the deactivator is introduced over the immobilized nano-metronomes. A sudden transition is clearly seen drastically changing the high FRET dwell time of the nano-metronome. Furthermore, E value of the high FRET state drops down from ~0.8 to ~0.6, which agrees with results shown in Figure 2C. Figure 4B shows the reverse process where we start the time trace with a silenced nano-metronome and flow in the activator strands at approximately t = 30 sec. Even though the activator strand contains a 5 nt region complementary to the overhang of strand X (see Supplementary figure S1), a transient 'intermolecular' interaction between them does not seem to affect the 'intramolecular' sticky end interactions significantly. Supplementary Figure S2 show more examples of these switching events. The whole process is consistently repeatable for several cycles hinting that the removal of the deactivator is complete and our nano-metronome can be reset over and over (data not shown).

Our nano-metronome can be further controlled to have different lifetimes in the low FRET state (*IsoI*). For example, instead of having just one pair of single stranded overhangs altering only the high FRET state dwell time, and an additional single stranded overhang can be added to the end of helix X so that basepairing between the overhangs on the helix X and helix B can be used to stabilize the low FRET state (Figure 5A). A representative time trace shows that this version of nano-metronome shows increased dwell times for both high and low FRET states.

We have demonstrated that a tunable nano-mechanical device, called the nano-metronome, can be constructed out of four single-stranded DNA molecules. Our nano-metronome is induced to tick by the ambient thermal energy and the rates of ticking is controlled by either the Mg^{2+} or by additional controlling elements, single stranded deactivator and activator. To our knowledge, this is the first demonstration of DNA-based nano-device observed at the single molecule level. We learned that even a single basepair difference in the sticky end can be easily detected and single molecular heterogeneity is small enough that even at the single nano-metronome level it should be possible to distinguish one basepair difference. Possible applications in the distant future may include the ultrasensitive detection of single nucleotide polymorphism.

We thank Adam Dally for experimental help and Robert Clegg for useful discussions. Funding was provided by an NSF CAREER Award, and a grant from the National Institute of Health (GM065367) to T.H. C.B. is a recipient of The Development and Promotion of Science and Technology Talents Project (DPST) Scholarship, Thailand and S.A.M. is an NSF graduate research fellow.

Supplementary Material

Refer to Web version on PubMed Central for supplementary material.

References

1. Yurke B, Turberfield AJAPM Jr, Simmel FC, Neumann JL. A DNA-fuelled molecular machine made of DNA. Nature 2000;406:605–608. [PubMed: 10949296]
2. Li JJ, Tan W. A Single DNA Molecule Nanomotor. Nano Letters 2002;2(4):315–318.
3. Chen Y, Wang M, Mao C. An Autonomous DNA Nanomotor Powered by a DNA Enzyme. Angewandte Chemie International Edition 2004;43:3554–3557.

4. Dittmer WU, Simmel FC. Transcriptional Control of DNA-Based Nanomachines. Nano Letters 2004;4 (4):689–691.
5. Alberti P, Mergny J-L. DNA duplex-quadruplex exchange as the basis for a nanomolecular machine. Proceedings of the National Academy of Sciences of the United States of America 2003;100(4):1569–1573. [PubMed: 12574521]
6. Mao C, Sun W, Shen Z, Seeman NC. A nanomechanical device based on the B-Z transition of DNA. Nature 1999;397:144–146. [PubMed: 9923675]
7. Liu D, Balasubramanian S. A Proton-Fuelled DNA Nanomachine. Angewandte Chemie International Edition 2003;42:5734–5736.
8. Liedl T, Simmel FC. Switching the Conformation of a DNA Molecule with a Chemical Oscillator. Nano Letters 2005;5(10):1894–1898. [PubMed: 16218705]
9. Viasnoff V, Meller A, Isambert H. DNA Nanomechanical Switches under Folding Kinetics Control. Nano Letters. In press
10. Yan H, Zhang X, Shen Z, Seeman NC. A Robust DNA mechanical device controlled by hybridization topology. Nature 2002;415:62–65. [PubMed: 11780115]
11. Feng L, Park SH, Reif JH, Yan H. A Two-State DNA Lattice Switched by DNA Nanoactuator. Angewandte Chemie International Edition 2003;42:4342–4346.
12. Tyagi S, Kramer FR. Molecular Beacons: Probes that Fluoresce upon Hybridization. Nature Biotechnology 1996;14:303.
13. Bonnet G, Krichevsky O, Libchaber A. Kinetics of conformational fluctuations in DNA hairpin-loops. Proceedings of the National Academy of Sciences of the United States of America 1998;95:8602–8606. [PubMed: 9671724]
14. Holliday R. A mechanism for gene conversion in fungi. Genetical Research 1964;5:282–304.
15. Lilley DMJ. Structures of helical junctions in nucleic acids. Qarterly Reviews of Biophysics 2000;33 (2):109–159.
16. Duckett DR, Murchie AIH, Diekmann S, Kitzing Ev, Kemper B, Lilley DMJ. The Structure of the Holliday Junction, and Its Resolution. Cell 1988;55:79–89. [PubMed: 3167979]
17. McKinney SA, Déclais A-C, Lilley DMJ, Ha T. Structural dynamics of individual Holliday junctions. Nature Structural Biology 2003;10(2):93–97.
18. Joo C, McKinney SA, Lilley DMJ, Ha T. Exploring Rare Conformational Species and Ionic Effects in DNA Holliday Junctions Using Single-molecule spectroscopy. Journal of Molecular Biology 2004;341:739–751. [PubMed: 15288783]
19. Grainger RJ, Murchie AIH, Lilley DMJ. Exchange between Stacking Conformers in a Four-Way DNA Junction. Biochemistry 1998;37:23–32. [PubMed: 9425022]
20. Clegg RM. Fluorescence resonance energy transfer. Methods in Enzymology 1992;211:353–388. [PubMed: 1406315]
21. Simmel FC, Yurke B. A DNA-based molecular device switchable between three distinct mechanical states. Applied Physics Letters 2002;80:883–885.

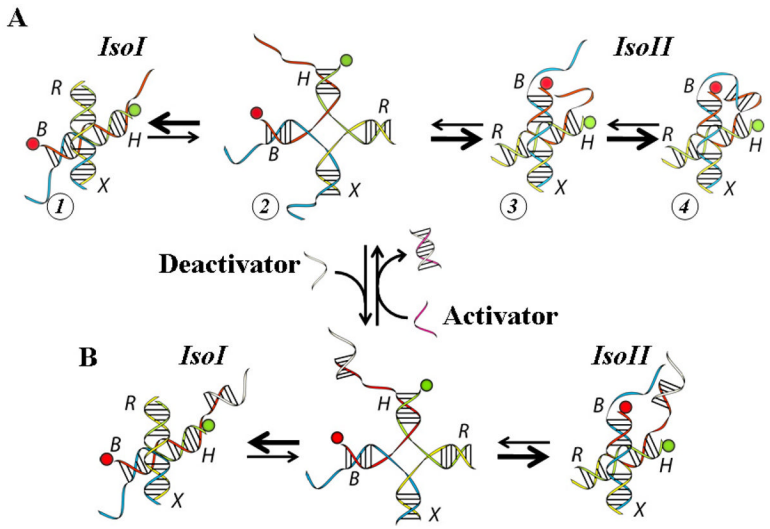

Figure 1.

(A) Diagram of conformational changes of a nano-metronome. In terms of native four-way Holliday junctions, s*tructure 1* possesses conformation *IsoI* whereas *structure 3* and *structure 4* possess conformation *IsoII*. The transition state s*tructure 2* reveals the sequence of each single stranded DNA. Basepairing of the sticky ends lowers the free energy of the *structure 4* forcing the nano-metronome to stay in conformation *IsoII* longer. The presence of Mg^{2+} is critical for the transitions to occur and the rates of transition depend on [Mg^{2+}] (see text) (B) Reversibly switching sticky ends on and off by utilizing the short single-stranded deactivator/activator. The deactivator competitively binds onto the single-stranded overhang at the end of helix H, silencing the sticky ends. This binding leaves an overhang handle for the activator to bind and later remove the deactivator via three-stranded branch migration.

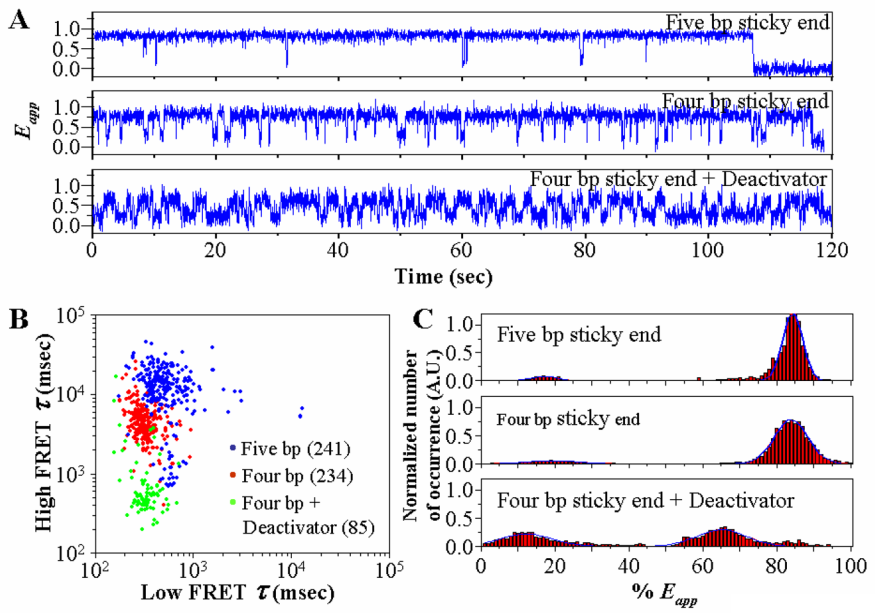

Figure 2.

(A) Sample FRET traces from nano-metronomes with five bp sticky end (top trace) four bp sticky end (middle trace) and silenced sticky end (bottom trace). The low FRET state corresponds to conformer *IsoI* and the high FRET state corresponds to the conformer *IsoII*. (B) A log-log plot of average high FRET (y axis) and low FRET (x axis) dwell times from the three groups of nano-metronomes. Each spot represents a single nano-metronome and the numbers in parenthesis in the figure legend indicate number of spots. (C) Normalized histogram plots of the apparent FRET efficiency ($E_{app}=\frac{\mathbf{I}_A}{\mathbf{I}_A+\mathbf{I}_D}$). The increase in FRET efficiencies of the high FRET state caused by the sticky ends (from $\boldsymbol{E}_{app} \approx 0.65$ in case of silenced sticky end to $\boldsymbol{E}_{app} \approx 0.83$ in case of four bp and five bp sticky end) indicates that the sticky ends bring two helical arms closer.

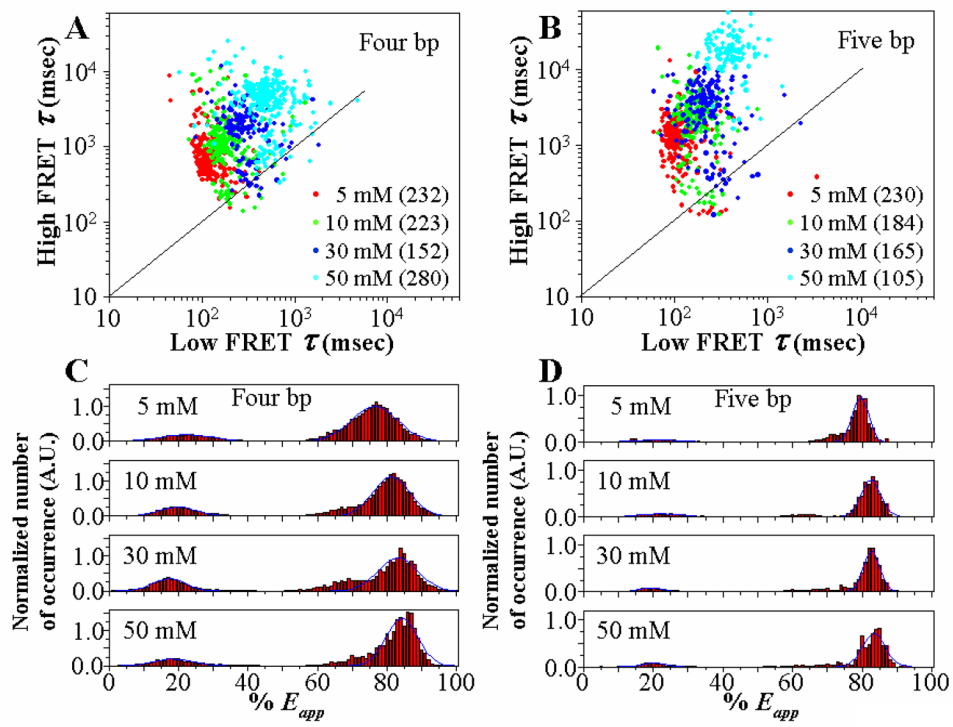

Figure 3.

Dependence of the high FRET and low FRET average dwell times on [Mg^{2+}] for nano-metronomes with four bp sticky end (A) and with five bp sticky end (B). The numbers in parenthesis indicates number of spots and the solid line marks a 1:1 ratio of the two native dwell times (found in Junction 7 without sticky ends). Larger deviation from the solid line suggests that Mg^{2+} might have a stronger effect on stabilizing the five bp sticky end. The increase in Mg^{2+} concentration correlates with the increase in the FRET values (C and D). There are two possible explanations for this behavior; one involves the junction itself and the other involves the stick end (see text for more details).

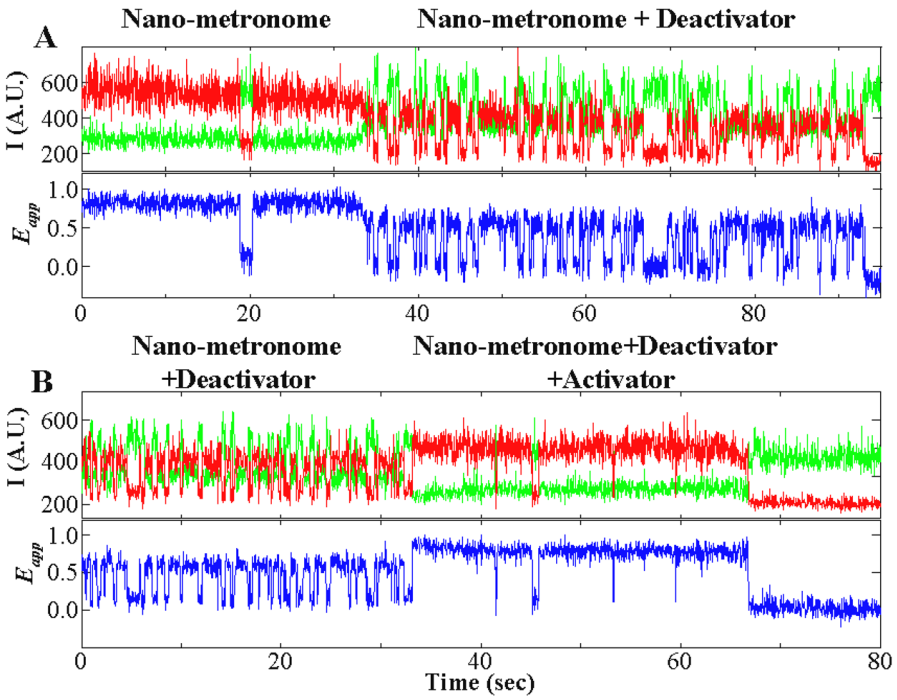

Figure 4.

Monitoring the sticky ends being deactivated (A) and re-activated (B) in real time using a flow delivery system. Because of the slow rate of hybridization, high concentrations (~ 1 μM) of both the deactivator and the activator are used to induce the transitions.

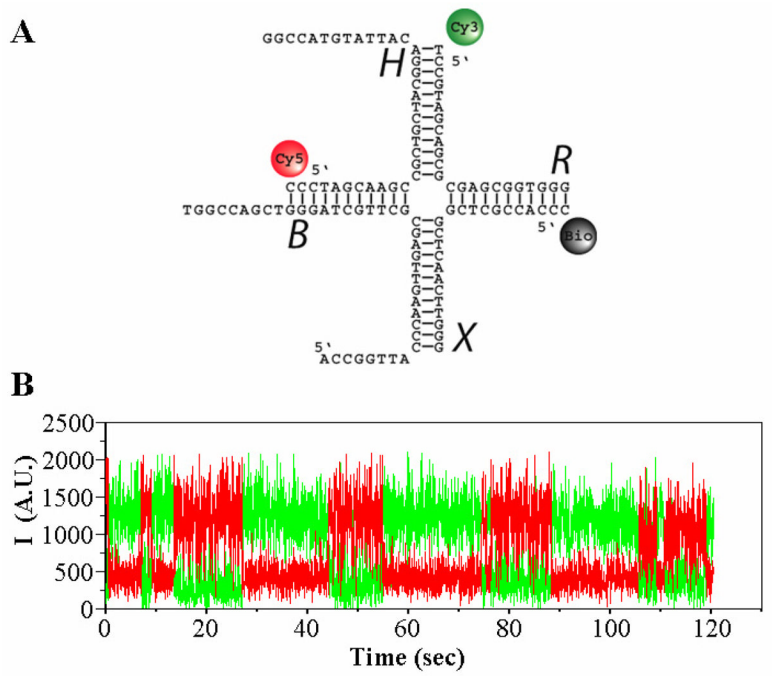

Figure 5.

Further modification of nano-metronome. (A) Addition of a third single-stranded overhang at the end of helix X could shift the bias of the dwell time toward *structure 1*. (B) A sample trace confirms the possibility.